Title:

The thermostability of a VADEX-Pro based protein nanoparticle

Ming-Chung Kan[1]

1. Vaxsia Biomedical Inc.

Abstract

We have adapted split GFP technology into the already established VADEX-based protein nanoparticle (PNP) platform. To evaluate this new platform, a model protein, maltose binding protein (MBP), was fused to the β-strand 11 of sfGFP and co-expressed with VADEX-10 that is composed of LYRRLE peptide and N-terminal part of sfGFP. When these two fusion proteins were expressed in a cell, they were assembled into PNP spontaneously with a DLS particle size of 26 nm. The thermostability of this PNP was verified by both SDS-PAGE and DLS analysis following thermal treatment. This PNP was stable at room temperature and at temperatures as high as 40 ^{o}C for at least two months. Mutations that replaced cysteine residue of the LYRRLE peptide with serine or alanine destabilized and induced degradation of the VADEX-based PNP. The results in this study showed that the non-covalent complementation of split sfGFP became irreversible when reconstituted sfGFP was assembled in a VADEX-based PNP. This platform may be applied in developing thermostable vaccines.

Introduction

Fluorescent proteins have been identified in jellyfishes, sea coral species and even arthropods(Alieva et al., 2008). These fluorescent proteins share one common barrel-can structure in which 11 β-strands enclose an alpha-helix that contains a three amino-acid chromophore. These β-strands provide structural support for precise spatial coordination that is needed for the maturation and functions of chromophore(Tsien, 1998). The fluorescent proteins have been applied in different fields: their applications including but not limited to serving as a marker for cell biological study; an indicatior for protein-protein interaction and as a monitor for proper folding of recombinant proteins(Cabantous et al., 2013; Pedelacq and Cabantous, 2019). Parts of the applications are based on split-GFP technology, in which these 11 β-strands of FP may be split into two or three uneven portions and they can be either expressed individually or been fused to two interacting proteins. And these split GFP portions can be reconstituted into a functional FP through strand complementation either through interacting between fusion partners or following thermodynamic interactions(Cabantous et al., 2005; Cabantous and Waldo, 2006).

In our previous study, we created a novel self-assembling protein nanoparticle (PNP)(Wong et al., 2023). This PNP was assembled from a fusion protein containing two modules: polymerization module and antigen presentation module. The polymerization module is a modified amphipathic helical peptide derived from the M2 protein of type A influenza virus strain H5N1. And the antigen presentation module is a superfolder green fluorescent protein (sfGFP) that is able to incorporate peptide onto the surface of PNP through loop insertion. When this fusion protein was expressed in cell, it self-assembled into PNP. We have identified gains of function mutant that provides thermostability to the PNP based on the protein models built on transmissive electronic microscope images. This technology is named VADEX-Πεπ, which stands for Vaccine Delivery system X-peptide. In this study, we have adapted split-GFP technology(Cabantous and Waldo, 2006) into VADEX-Pep and created a new platform, VADEX-Pro, that is able to incorporates large antigen onto the surface of VADEX-based PNP. We evaluated the thermostability of the PNP assembled by VADEX-pro expressing MBP using both DLS and SDS-PAGE.

Results

The design of the VADEX-Pro protein nanoparticle.

The limitation on the size of peptide that can be inserted into the sfGFP loop poses a significant problem when developing subunit vaccines using the VADEX technology created in our previous study. In order to express large antigen on the surface of VADEX-based nanoparticle, we have adopted split-GFP technology for incorporating large protein onto a VADEX-based nanoparticle. We fused the N-terminal of sfGFP that contains β-strand 1-10 to the

C-terminal of polymerization peptide, LYRRLE, and generated the fusion protein, VADEX-10. The complementary β-strand 11 of sfGFP was fused to the C-terminal of a target antigen, the maltose binding protein (MBP) cloned from a protein expression vector, pD-MAL1, and the fusion protein is named as MBP-11. These two fusion proteins were co-expressed in *E.coli* by constructing both ORFs in the same pET-Duet1 vector (Figure 1A). The PNP that was assembled by fusion proteins encoded in this vector was named as MBP-C in this study. When we analyzed the protein expression profile that expressed only the targe antigen, MBP-11, or both VADEX-10 and MBP-11, we found the co-expression of complementary fusion proteins is able to stabilize fusion proteins when comparing soluble fractions from bacteria expressing either single or both fusion proteins (Figure 1B). The his-tag for protein purification was fused only to the MBP-11 so the only possibility that VADEX-10 can be purified by a Ni-NTA resin is because it was assembled into PNP with MBP-11 through strand complementation (Figure 1B).

The cysteine 8 (Cys8) residue in the polymerizing peptide, LYRRLE, has been predicted to mediate the formation of hydrogen bonds between two stacking dimers in the VADEX protein nanoparticle according to a protein model that was built on TEM images. To test the role of the Cys8 in the stability of the VADEX-based protein nanoparticle, we made point mutants of LYRRLE peptide by replacing the Cys8 with either serine (MBP-S) or alanine (MBP-A) in the MBP-C expression vector and examined the stability of nanoparticles that were assembled by the LYRRLE and the mutant peptides. The expression of MBP-C PNP reached 50 mg/L in flask culture and the mutants also have similar expression level (unpublished result). Similar to the previous study, we found that the VADEX PNPs that expressed MBP on surface was stable in elution buffer at cold room storage for at least one month (Figure 1C). When the storage buffer was replaced with phosphate buffer (pH 8.0) with 150 mM NaCl, the MBP-S PNP became unstable in room temperature and the MBP-11 was degraded or precipitated within the first two weeks. The MBP-A PNP was more stable than the MBP-S PNP, but it was hydrolyzed into smaller size at the second month. The MBP-C PNP was stable for more than one month before showing signs of protein hydrolysis (Figure 2A). The stability of MBP-C PNP was also supported by Dynamic Light Scattering (DLS) analysis. The Z average diameter of PNP assembled from wildtype peptide (MBP-C) was 26.36 nm and was shown as a single peak (Figure 2B, left panel). Whereas the DLS profile of MBP-A mutant has two peaks of different size (Figure 2C, left panel) and the first peak matched with the DLS profile of MBP-11 (Figure 2D, right panel), suggests the purified MBP-A PNP containing two populations, assembled PNP and dissociated MBP-11 proteins. For MBP-C PNP, after been incubated in RT for 2 months, the MBP-C particle remains intact with more variation in particle size (Figure 2B, right panel). For MBP-A PNP, the percentage of dissociated MBP-11 protein has increased from 55.2% to 71.1% after 2 months storage in RT (Figure 2C, right panel).

The β-strand complementation of sfGFP was reported as irreversible unless under the condition of photo-dissociation (Lin et al., 2017). The results from evaluating the stability of MBP-C PNP and its variants at RT storage underscore the significance of Cys8 in LYRRLE peptide mediated PNP assembly. To test the thermostability of MBP-C and MBP-A PNPs in higher temperature, we incubated both PNPs in a series of elevated temperatures each for one hour and then verified the structural integrity of sfGFP by fluorescence imaging and particle stability by DLS analysis. Both MBP-C and MBP-A PNP lost fluorescence when the temperature reached 80 ^{o}C (Figure 3A), which is consistent with previous reports on the thermostability of split-GFP and sfGFP (Frenzel et al., 2018; Pédelacq et al., 2006). The Z average diameter of MBP-C PNP increased by 50% when the temperature was elevated from 40 ^{o}C to 50 ^{o}C, whereas the particle size of MBP-A PNP increased by 3 folds under same conditions (Figure 3B). At 70 ^{o}C, the particle size from both samples reached their peaks. Considering the apparent stability of MBP-C in room temperature and particle integrity after storage, we decided to focus on MBP-C when testing the long-term thermostability of VADEX-based PNP. In previous study, the salt concentration in storage buffer was found to affect the stability of VADEX-based PNP (Wong et al., 2023). To test the effects of NaCl concentration on MBP-C PNP long-term thermostability, the NaCl concentration in storage buffer was adjusted to either 300 mM, 600 mM, or 900 mM and PNPs were then maintained at either 40 ^{o}C or 50 ^{o}C and folllowed for 8 weeks. The thermostability of PNP was monitored in three categories: the protein integrity was evaluated by SDS-PAGE; the particle size was determined by DLS; the concentration of PNP remained as soluble form was measured by UV 280 nm.

When the MBP-C PNP was incubated at 40 ^{o}C, the particle size was relatively stable with an increase of Z average diamteter ranged between 24.4 % (150 mM NaCl) to 49.7 % (600 mM NaCl) after 8 weeks. But when the PNP was incubated in 50 ^{o}C, the Z average diameter of MBP-C PNP increased dramatically within one day by 3.3 to 7.7 folds (Figure 3C). This dramatic increase in particle size was correlated with the precipitation and removal of PNP from solution within two weeks (Figure 3F, 3G). These data suggested the MBP-C PNPs were stable at 40 ^{o}C storage for at least two months without showing significant PNP particle change in size or protein lost to denaturation. Whereas when these PNPs were stored at 50 ^{o}C, the half-life is less than 14 days due to protein denaturation and precipitation, a result that was similar among MBP-C PNP in different NaCl concentrations (Figure 3G). In contrast, when MBP-C PNP were stored at 4 ^{o}C, both VADEX-10 and MBP-11 were hydrolyzed into smaller fragments (marked with asterisk) after stored in the buffers containing either 150 mM or 300 mM NaCl at 4 ^{o}C for two months. The MBP-C PNP stored in buffers containing 600 mM or 900 mM NaCl is more stable and only partially hydrolyzed (Figure 3H). This result suggests that the MBP-C PNP degradation at 4 ^{o}C and 50 ^{o}C are through different pathways. But the result is consistant with previous study that VADEX-based

protein nanoparticle is stabilized by the presence of high salt that strengthened hydrophobic interactions within the PNP(Wong et al., 2023).

Discussion:

In this study, we have shown that a large protein like maltose binding protein, MBP, can be incorporated onto the VADEX-based PNP through sfGFP strand complementation. The assembled PNP is stable at room temperature and at 40 ^{o}C for at least two months and the reconstituted sfGFP can withstand high temperature incubation in the same level like full length sfGFP. These results suggested that the strand complementation that the VADEX-Pro use to incorporate large antigen onto PNP is likely irreversible when the reconstituted sfGFP was assembled into a multimeric PNP. In contrast, when the stucture of MBP-C PNP was weaken by the substitution of Cys8 by alanine or been stored in 4 ^{o}C, complemented sfGFP falls apart and dissociated antigen increases over time as expected for proteins bound by non-covalent methodology.

When stored at higher temperature, MBP-C PNPs were aggregated non-specifically into large particles and precipitated in a salt-independent manner. This salt-independent aggregation maybe due to the partial denaturation of MBP, which has a Tm of 64.9 ^{o}C, because of the difference of PNP deterioration patterns between high temperature incubation and Cys8 substitution or cold temperature storage. The overall stability of a PNP depends on the less stable component of the particle. In our previous study, the unstructured peptide antgen (hM2e) became the target of water hydrolysis even when the particle size remain stable (Wong et al., 2023). Although other factors besides structural integrity, like zeta-potential or salt strength are also important for the stability of PNP under high temperature (Samandoulgou et al., 2015). The MBP used in this study was cloned from pD-MAL1 vector with an isoelectric point (pI) of pH 4.9, that will create a large zeta-potential for preventing PNP aggregation in a phosphate buffer (pH 8.0) used in this study. The hydrolysis of MBP-C PNP in 4 ^{o}C storage under salt concentration dependency is consistant to previous study(Wong et al., 2023). This data suggested that the storage in low temperature may alters the structure of LYRRLE peptide and reduces its ability to assemble into PNP tightly, a caveate that can be compensated by using buffer with higher NaCl concentration.

In the previous study, cys8 in the LYRRLE peptide was predicted to form a hydrogen bond with the glutamic acid from another dimer and stabilizing the PNP. In this study, we provide further evidence showing the significance of cys8 in VADEX PNP stability. After cysteine was replaced with serine or alanine, the PNP become unstable or unable to form PNP of proper size. The MBP-S has a large particle size, z average diameter=600 nm, that is 20 folds more than the size of MBP-C particle and it was quickly degraded. The MBP-A PNP has a similar particle size as MBP-C, but the fusion protein falls into two peaks in DLS analysis. The smaller peak shares the

same DLS profile with MBP-11 and it suggests the MBP-A fusion proteins fall into two populations, the assembled and disassembled proteins and the disassembled proteins are prone to hydrolysis. So, the substitution of cysteine with alanine or serine in LYRRLE peptide reduces the stability of the PNP.

In conclusion, we have adapted split-GFP technology in VADEX PNP and enabled the incorporation of large proteins onto the surface of VADEX PNP through irreversible strand complementation and this platform may serves as a basis for developing thermostable vaccines.

Methods and materials

Plasmid construction

The VADEX-10 and strand 11 of sfGFP were synthesized by GeneArt. The VADEX-10 coding DNA were digested by NdeI and SalI and ligated with pET-Duet1 vector digested with NdeI and XhoI and the result plasmid is named VADEX-10. The strand 11 of sfGFP was digested by SalI and NotI and was ligated with the VADEX-10 that has been digested by SalI and NotI and the result plasmid was named VADEX-Pro. The maltose binding protein coding region was PCR amplified from pD-MAL1 and inserted into the VADEX-Pro vector N-terminal in frame to the strand 11 or sfGFP between EcoRI and PstI. Site directed mutagenesis of cysteine 8 was introduced by primers containing point mutations to the LYRRLE coding region.

Protein expression, purification and analysis

Protein expression and purification have been described in detail in previous report. In short, the MBP-C PNP and its variants were expressed in Clearcoli strain containing DE3 transposon. After protein expression, PNPs were purified using Ni-NTA resin and eluted, stored at 4 ^{o}C in elution buffer (20 mM Na(PO_4), 300 mM NaCl and 500 mM Imidazole pH 8.0). Before thermostability test, the storage buffer of PNPs were changed from elution buffer to ½x storage buffer (10 mM Na(PO4), 150 mM NaCl pH 8.0) and NaCl were adjusted to designated concentration if necessary. DLS analysis was carried out in Stunner (Unchained Labs, Pleasanton CA). For thermostability test, PNPs were incubated in PCR block with continuous thermal control.

Figure 1.

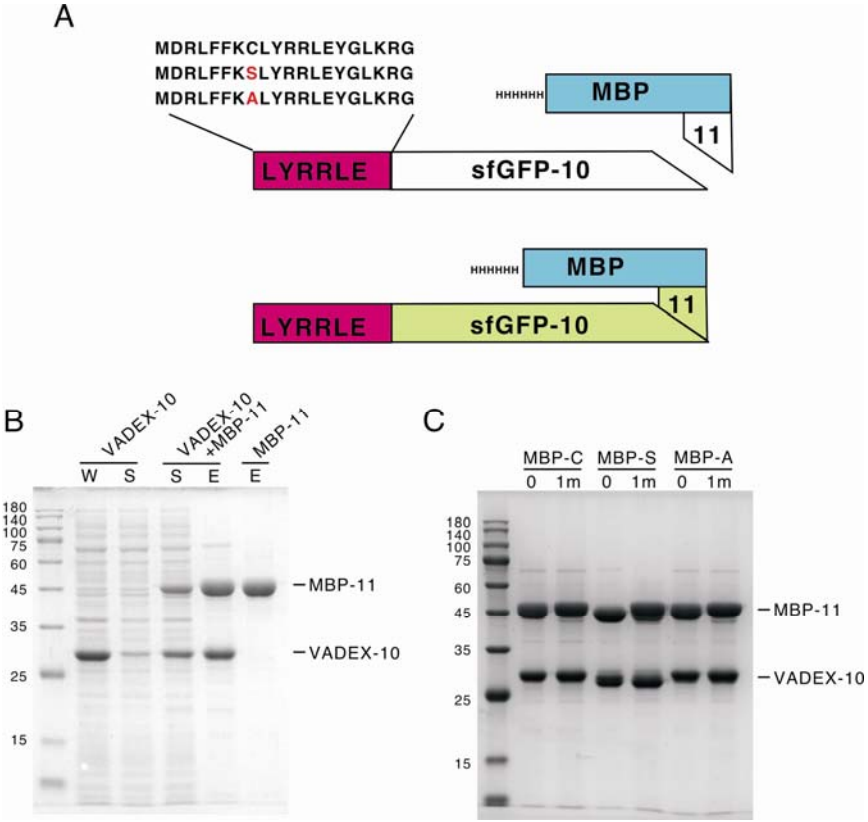

Figure 1. The design and protein expression of VADEX-Pro protein nanoparticle and its variants. A) The N-terminal part of sfGFP containing β-strand 1-10 was fused to the C-terminal of polymerization module, LYRRLE, and the fusion protein was named as VADEX-10. The β-strand 11 of sfGFP was fused to the C-terminal of a model protein, maltose binding protein (MBP), and the fusion protein was named MBP-11. These two fusion proteins were co-expressed from the same expression vector, pET-Duet-1. The PNP that assembled from these two fusion proteins was named as MBP-C in this study. The cysteine residue in the LYRRLE peptide of MBP-C was replaced by either serine or alanine and the PNP were renamed as either MBP-S or MBP-A, respectively. B) The whole cell lysate (W), soluble fraction (S), or eluted protein (E) from bacteria expressing either VADEX-10, MBP-11 or both fusion proteins were analyzed by SDS-PAGE. C) The purified MBP-C PNP and its variants, MBP-S, and MBP-A PNPs were analyzed by SDS-PAGE. The protein nanoparticles eluted from Ni-NTA resin were stored in elution buffer for one month before SDS-PAGE analysis to evaluate the stability of protein nanoparticles in elution buffer.

Figure 2.

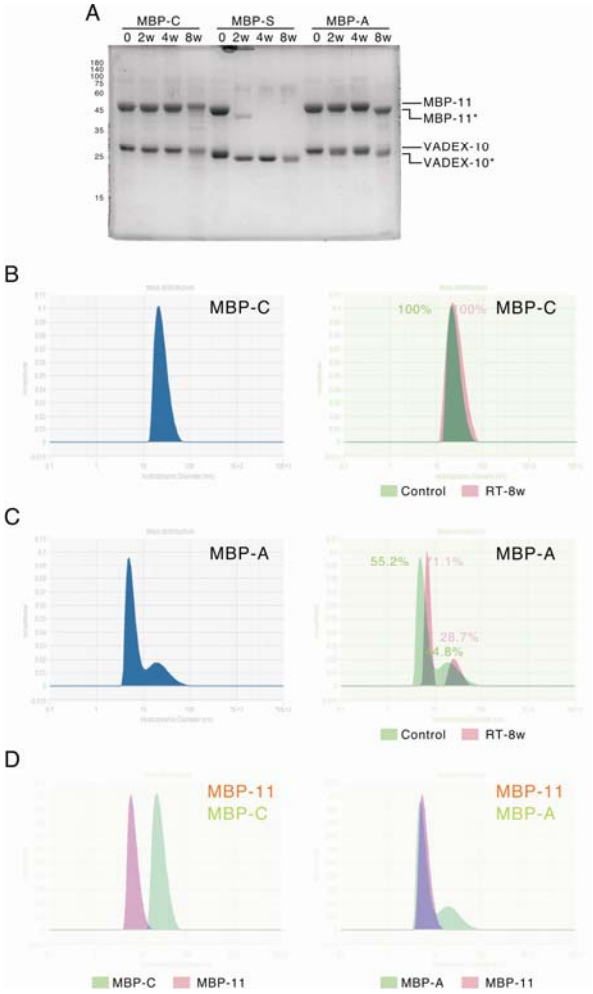

Figure 2. The stability of MBP-C and its variants in room temperature storage in physiological buffer. A) MBP-C PNP and its variants were stored in room temperature for up to two months and protein samples were taken in designated time point for analysis for protein integrity by SDS-PAGE. The hydrolyzed MBP-11 and VADEX-10 fusion proteins were marked by an asterisk "*". B) The stability of MBP-C and MBP-A PNPs were analyzed by DLS for particle stability in room temperature storage. The left panel were DLS results from protein samples one hour after the storage buffer was changed to phosphate buffer containing 150 mM NaCl using desalting column. The right panels were the result after merging left panel with DLS result from MBP-C PNP that has been stored for 2 months in room temperature. DLS result from control PNP were shown as green and the result from PNP been stored at room temperature for two months were shown in pink. C) The same DLS analysis results of MBP-A PNP were shown. D) The comparisons of MBP-C and MBP-A DLS results to that of MBP-11 were shown. The merged DLS results from

MBP-C and MBP-11 was shown in the left panel. The merged DLS results from MBP-A and MBP-11 was shown in the right panel.

Figure 3.

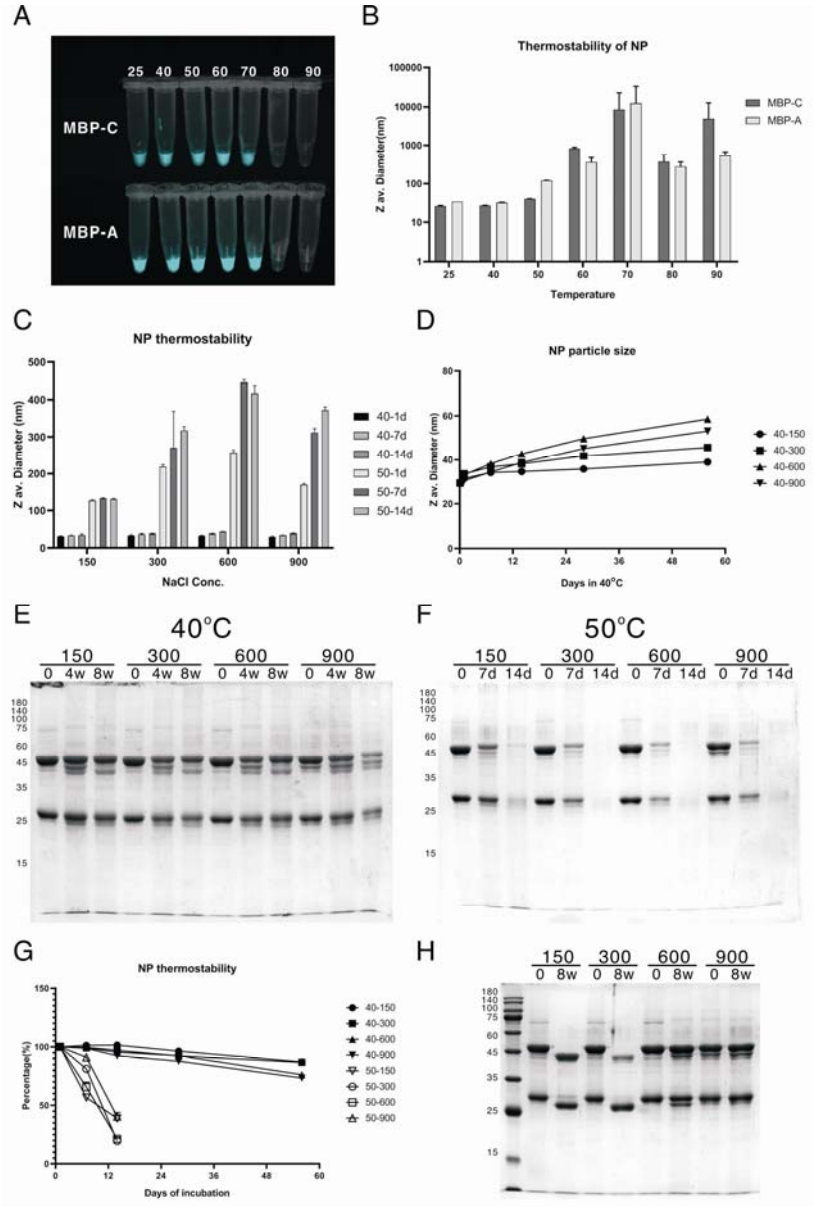

Figure 3. The thermostability of MBP-C protein nanoparticles. A) The fluorescence of MBP-C and MBP-A PNPs after been incubated in a series of elevated temperatures for one hour. B) The Z average diameter (Z av diameter) of MBP-C and MBP-A PNPs after been incubated in different temperatures for one hour were compared. (N=3) C) The Z average diameter of MBP-C protein nanoparticles incubated in 40 ^{o}C or 50 ^{o}C for a time period up to 14 days in storage buffers containing different NaCl concentration were shown. (N=3) D) The hydrodynamic particle size of

protein nanoparticle incubated in phosphate buffer containing either 150 mM, 300 mM, 600 mM, or 900 mM NaCl at 40 ^{o}C were followed for 8 weeks. (N=3) E) The integrity of protein nanoparticles stored in phosphate buffer containing 150 mM, 300 mM, 600 mM, or 900 mM NaCl at 40 ^{o}C was followed for a time period up to 8 weeks. The protein samples were collected at designated time points and stored in -20 ^{o}C before been analyzed by SDS-PAGE. F) The same experimental design as in Fig. 3E, except the storage termperature was 50 ^{o}C. G) The concentration of protein nanoparticle remained in solution after been stored in either 40 ^{o}C or 50 ^{o}C were followed for 8 weeks. H) The MBP-C PNP in phosphate buffer containing different concentration of NaCl were stored in 4 ^{o}C for 2 months and the protein integrity was analyzed by SDS-PAGE.

References:

Alieva, N.O., Konzen, K.A., Field, S.F., Meleshkevitch, E.A., Hunt, M.E., Beltran-Ramirez, V., Miller, D.J., Wiedenmann, J., Salih, A., and Matz, M.V. (2008). Diversity and evolution of coral fluorescent proteins. PLoS One *3*, e2680.

Cabantous, S., Nguyen, H.B., Pedelacq, J.D., Koraichi, F., Chaudhary, A., Ganguly, K., Lockard, M.A., Favre, G., Terwilliger, T.C., and Waldo, G.S. (2013). A new protein-protein interaction sensor based on tripartite split-GFP association. Sci Rep *3*, 2854.

Cabantous, S., Terwilliger, T.C., and Waldo, G.S. (2005). Protein tagging and detection with engineered self-assembling fragments of green fluorescent protein. Nat Biotechnol *23*, 102-107.

Cabantous, S., and Waldo, G.S. (2006). In vivo and in vitro protein solubility assays using split GFP. Nat Methods *3*, 845-854.

Frenzel, E., Legebeke, J., van Stralen, A., van Kranenburg, R., and Kuipers, O.P. (2018). In vivo selection of sfGFP variants with improved and reliable functionality in industrially important thermophilic bacteria. Biotechnol Biofuels *11*, 8.

Lin, C.Y., Both, J., Do, K., and Boxer, S.G. (2017). Mechanism and bottlenecks in strand photodissociation of split green fluorescent proteins (GFPs). Proc Natl Acad Sci U S A *114*, E2146-E2155.

Pedelacq, J.-D., and Cabantous, S. (2019). Development and Applications of Superfolder and Split Fluorescent Protein Detection Systems in Biology. International journal of molecular sciences *20*, 3479.

Pédelacq, J.-D., Cabantous, S., Tran, T., Terwilliger, T.C., and Waldo, G.S. (2006). Engineering and characterization of a superfolder green fluorescent protein. Nature Biotechnology *24*, 79-88.

Samandoulgou, I., Fliss, I., and Jean, J. (2015). Zeta Potential and Aggregation of Virus-Like Particle of Human Norovirus and Feline Calicivirus Under Different Physicochemical Conditions. Food Environ Virol *7*, 249-260.

Tsien, R.Y. (1998). THE GREEN FLUORESCENT PROTEIN. Annual Review of Biochemistry *67*, 509-544.

Wong, T.-T., Liou, G.-G., and Kan, M.-C. (2023). A Thermal-Stable Protein Nanoparticle That Stimulates Long Lasting Humoral Immune Response. Vaccines *11*, 426.